

Experimental Study on Thermomechanical Properties of New-Generation ODS Alloys

O. Khalaj, B. Mašek, H. Jirková, J. Svoboda

Abstract—By using a combination of new technologies together with an unconventional use of different types of materials, specific mechanical properties and structures of the material can be achieved. Some possibilities are enabled by a combination of powder metallurgy in the preparation of a metal matrix with dispersed stable particles achieved by mechanical alloying and hot consolidation. This paper explains the thermomechanical properties of new generation of Oxide Dispersion Strengthened alloys (ODS) within three ranges of temperature with specified deformation profiles. The results show that the mechanical properties of new ODS alloys are significantly affected by the thermomechanical treatment.

Keywords—Hot forming, ODS, alloys, thermomechanical, Fe-Al, Al_2O_3 .

I. INTRODUCTION

NEW unconventional structure with specific mechanical and physical properties with new application possibilities in some areas of industry can be obtained using conventional materials through innovative technological techniques. A notable improvement in the field was made by J. S. Benjamin at the International Nickel Company (INCO) laboratory: he proposed a new process based on high energy milling powder metallurgy – later called mechanical alloying [1], [2]. This process was introduced to obtain a fine and homogeneous oxide dispersion within a nickel matrix.

Currently, mechanical alloying is still considered to be the most effective process for obtaining fine and homogeneously distributed particles [3], [4]. The volume fraction of dispersed spherical oxides (usually Y_2O_3) is typically below 1% [5], [6], and the oxides typically have a mean size of 5-30 nm [7]-[9]. Based on the thermomechanical analysis, this paper presents the development of new ODS Fe-Al based alloys applicable at high temperatures up to about 1200 °C. The new ODS alloy consists of a ferritic Fe-Al matrix strengthened with 6-10 vol.% of Al_2O_3 particles. The new ODS alloys produced by combination of mechanical alloying [10], [11] and hot consolidation [12], [13] are new types of materials with a promising property spectrum [14], [15]. The experimental program was carried out in order to get a more detailed insight into this new group of materials, to better understand their

O. Khalaj is with the Research Centre of Forming Technology, University of West Bohemia, Univerzitní 22, 306 14, Pilsen, Czech Republic (corresponding author, phone: +420-776077346; e-mail: khalaj@vctt.zcu.cz).

B. Mašek and H. Jirková are with the Research Centre of Forming Technology, University of West Bohemia, Univerzitní 22, 306 14, Pilsen, Czech Republic (e-mail: masekb@vctt.zcu.cz, hstankov@vctt.zcu.cz).

J. Svoboda is with the Institute of Physics of Materials, Academy of Sciences of the Czech Republic, Žitkova 22, 616 62, Brno, Czech Republic (e-mail: svobj@ipm.cz).

processing behaviour and their operational properties.

II. PREPARATION OF ODS ALLOYS

Mechanically alloyed (MA) powders were prepared in a low energy ball mill developed by the authors, which enables evacuation and filling by oxygen. The MA powders consisting of Fe10wt.%Al matrix and 6-10 vol. % of Al_2O_3 particles were deposited into a steel container of diameter 70 mm, evacuated and sealed by welding. The steel container was heated up to a temperature of 800-900 °C and rolled by a hot rolling mill to a thickness of 20-25 mm in the first rolling step and then heated up to a temperature of 1100 °C and rolled to a thickness of 9 mm in the second step. The final production is 6 mm thick sheet of the ODS alloy which is sent to cutting system for preparation of samples. Afterwards, the specimens were cut by water jet to a standard pretested shape.

III. EXPERIMENTAL PROCEDURE

In order to investigate the thermomechanical treatment of specimens, a servohydraulic MTS thermomechanical simulator (Fig. 1) was used, which allows running of various temperature-deformation paths, different numbers of deformation, strain rate and temperatures. It also capable of applying combined tensile and compressive deformation which leads to increase in plastic deformation (and a high dislocation density) in the specimen.

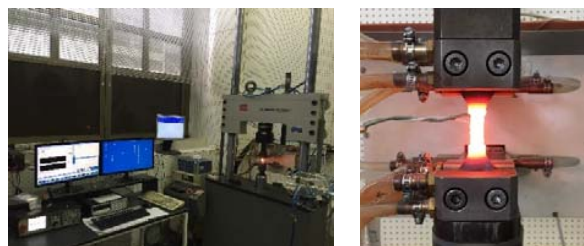


Fig. 1 Treatment on thermomechanical simulator

Four types of material were used in this research as described in Table I. All these materials are based on Fe10wt.% Al ferritic matrix with different particle size and vol.% of Al_2O_3 . Al_2O_3 powder was added to prepare the composite which leads to internal oxidation during mechanical alloying and hot consolidation. SEM analysis shows some inhomogeneities which occurred due to sticking of the material during mechanical alloying on the walls of the milling container. It could have some influence on the mechanical properties of materials; however; the mechanical

alloying process is steadily optimized with respect to the homogeneity of the materials.

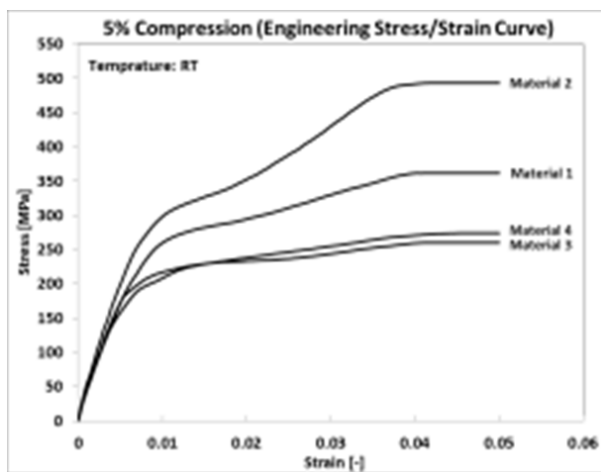
TABLE I
MATERIAL PARAMETERS

| Mat. No. | Material Type | Milling time [hours] | Ferritic Matrix | Vol.% of Al ₂ O ₃ | Typical Particle Size [nm] |
|----------|---------------|----------------------|-----------------|---|----------------------------|
| 1 | Composite | -- | Fe10wt.%Al | 10 | 300 |
| 2 | ODS Alloy | 100 | Fe10wt.%Al | 6 | 50-200 |
| 3 | ODS Alloy | 150 | Fe10wt.%Al | 6 | 50-150 |
| 4 | ODS Alloy | 200 | Fe10wt.%Al | 6 | 30-150 |

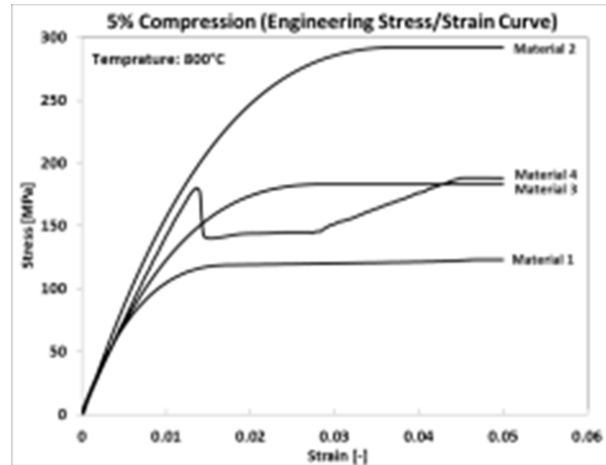
The tests were carried out to investigate the thermomechanical behaviour of the different materials (1 to 4) at different temperatures regarding single loading with constant strain rate of 1 s^{-1} . In order to give a clearer comparison of the results, only the results at room temperature (RT), 800 °C, and 1200 °C are presented.

IV. RESULTS AND DISCUSSION

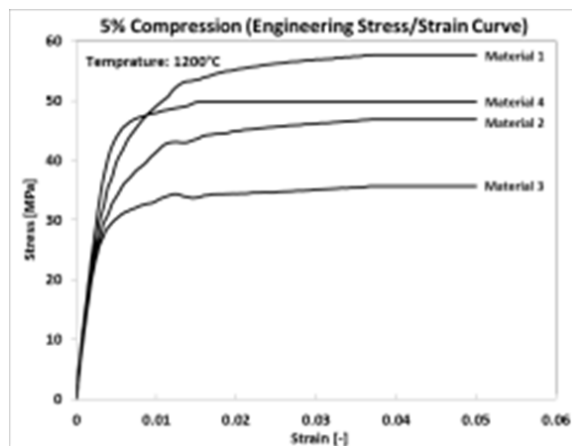
Fig. 2 shows the stress-strain curves for all materials at different temperatures regarding the 5% compression corresponding to treatment number 1. Material 2 exhibits a better strength at 30 °C and 800 °C, but at 1200 °C Material 1 shows a better strength. Hot working behaviour of alloys is generally reflected by flow curves, which are a direct consequence of microstructural changes: the nucleation and growth of new grains, dynamic recrystallization (DRX), generation of dislocations, work hardening (WH), rearrangement of dislocations and their dynamic recovery (DRV). Besides, the flow curve for Material 4 was somehow strange, so it repeated several times; however, it shows the same pattern. It could be concluded that it happens because of the inhomogeneity of the microstructure of this material.



(a)



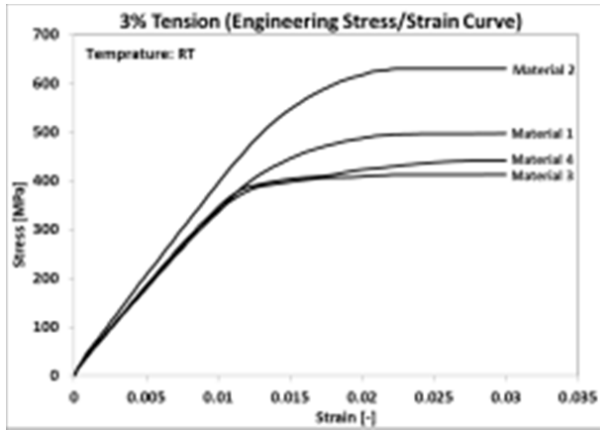
(b)



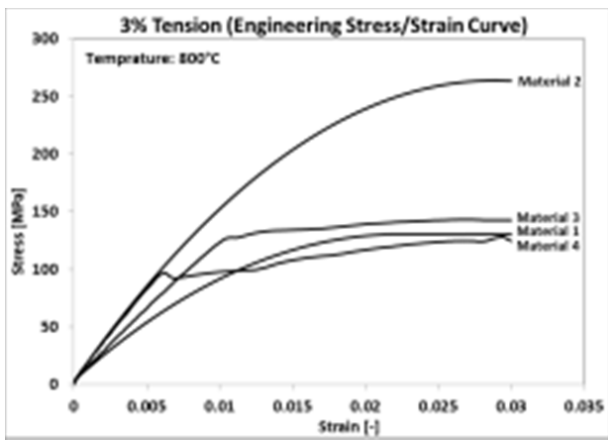
(c)

Fig. 2 Stress-strain curves (5% compression) for (a) RT, (b) 800 °C, (c) 1200 °C

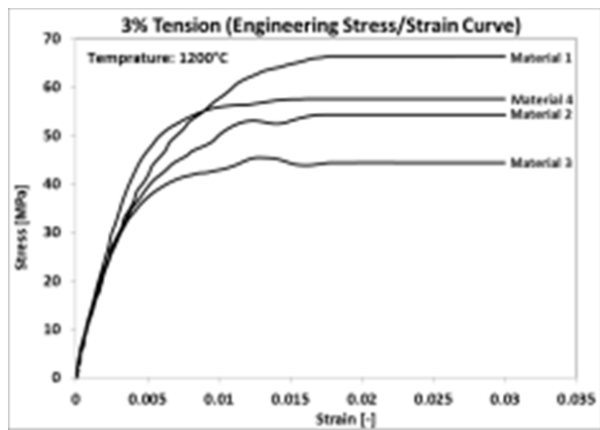
Fig. 3 shows the stress-strain curves for materials 1 to 4 at different temperatures corresponding to the 3% tension. As it can be seen in Fig. 3, material 2 shows a higher strength at 30 °C and 800 °C but at 1200 °C, again material 1 shows a better strength. The maximum stress and trends of curves show sensitivity to the deformation temperatures changes. Thus, by lowering temperature, the yield stress level increased. In the other words, it prevents the occurrence of softening due to DRX and DRV and allows the deformed metals to exhibit WH.



(a)



(b)



(c)

Fig. 3 Stress-strain curves (3% tension) for (a) RT, (b) 800 °C, (c) 1200 °C

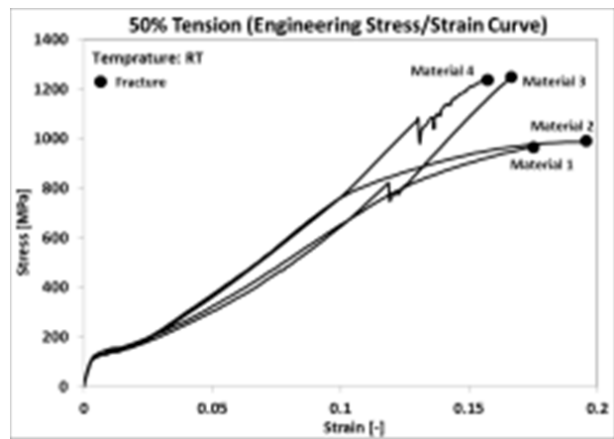
at 800 °C the same as Material 1 and 2 at 1200 °C. The trends of flow curves show three distinct stages.

Hardening predominates in the first stage and causes dislocations into stable subgrains. Flow stress exhibits a rapid increase with increasing strain up to a critical value. Then, regarding to large differences in dislocation density, recrystallization happened within subgrains or grains, and new grains are nucleated along the grain boundaries which leads to larger grains.

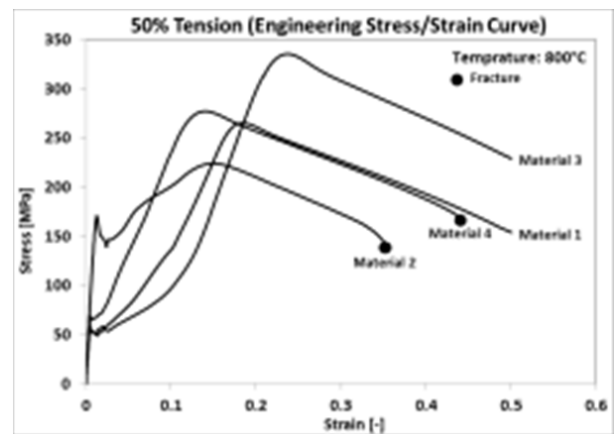
In the next stage, it shows the thermal softening due to DRX and DRV, which becomes more and more important and they nearly compensate hardening.

By the last stage, three types of curves can be recognized:

- Increasing continuously with significant work-hardening (Fig. 4 (a))
- Increasing gradually to a steady state with hardening (Fig. 4 (b))
- Decreasing continuously with significant DRX softening (Fig. 4 (c)).

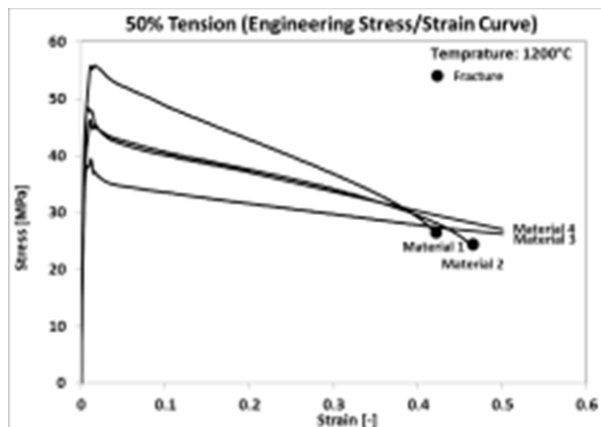


(a)



(b)

Fig. 4 shows the stress-strain curves for materials 1 to 4 at different temperatures corresponding to 50% tension. Except material 3 and 4, all materials failed below 50% tension at 1200 °C; however, all the four materials failed at RT. It can be seen that Material 2 and Material 4 failed at almost 40% strain



(c)

Fig. 4 Stress-strain curves (50% tension) for (a) RT, (b) 800 °C, (c) 1200 °C

V. CONCLUSION

This paper outlines the results of characterization of the single and multiple deformation thermomechanical behaviour of a new generation of ODS alloys. Four materials differing from each other in the amount and size of the oxides embedded in the ferritic matrix were tested under different conditions. The advantages of all the materials are their low-cost and oxidation-resistance. The oxide dispersion significantly strengthens the material; however, the typical form of the flow curve with DRX softening, including a single peak followed by a steady state flow as a plateau, is more recognizable at high temperatures than at low temperatures. This is because at high temperatures the DRX softening compensates the WH, and both the peak stress and the onset of steady state flow came to lower strain levels. The behaviour of four materials under different heat treatment can be summarized as follows:

- 1) The maximum stress and trends of curves show sensitivity to the deformation temperatures changes. In the other words, it prevents the occurrence of softening due to DRX and DRV and allows the deformed metals to exhibit WH.
- 2) All the flow curves show decreasing to a steady state after rapid increase in the stress to maximum value. Differences in softening rate usually depend on DRX and the stress evolution with strain within different stages.
- 3) In all tests, the elastic strain was higher than plastic strain even for the total strain of 15%, which confirms strengthening the materials within oxide particle effect.

ACKNOWLEDGMENT

This paper includes results created within the projects 17-01641S Improvement of Properties and Complex Characterization of New Generation Fe-Al-O Based Oxide Precipitation Hardened Steels subsidised by the Czech Science Foundation, and SGS-2016-060 Research of Modern AHS Steels and Innovative Processes for their Manufacturing subsidised from specific resources of the state budget for

research and development

REFERENCES

- [1] Inco Alloys Limited, Material data sheet, INCOLOY, alloy MA 956, INCOLOY, alloy MA 957, Hereford, U.K.
- [2] W. Quadackers, Oxidation of ODS alloys. *Journal de Physique IV*, 03 (1993) C9, 177- 186.
- [3] F. D. Fischer, J. Svoboda, P. Fratzl, A thermodynamic approach to grain growth and coarsening, *Journal of Philosophical Magazine*, 83 (2003) 9, 1075–1093.
- [4] F. Pedraza, Low Energy-High Flux Nitridation of Metal Alloys: Mechanisms, Microstructures and High Temperatures Oxidation Behaviour, *Materials and technology*, 42 (2008) 4, 157-169M. Young, the Technical Writers Handbook. Mill Valley, CA: University Science, 1989.
- [5] O. Khalaj, B. Mašek, H. Jirkova, A. Ronesova, J. Svoboda, Investigation on New Creep and Oxidation Resistant Materials, *Materials and technology*, 49 (2015) 4, 173-179.
- [6] M. J. Alinger, G. R. Odette, D. T. Hoelzer, On the role of alloy composition and processing parameters in nanocluster formation and dispersion strengthening in nanostructured ferritic alloys, *Acta Material*, 57 (2009) 2, 392-406.
- [7] P. Unifantowicz, Z. Oksiuta, P. Olier, Y. de Carlan, N. Baluc, Microstructure and mechanical properties of an ODS RAF steel fabricated by hot extrusion or hot isostatic pressing, *Fusion Engineering and Design*, 86 (2011), 2413–2416.
- [8] M.A. Auger, V. de Castro, T. Leguey, A. Muñoz, R. Pareja, Microstructure and mechanical behavior of ODS and non-ODS Fe-14Cr model alloys produced by spark plasma sintering, *Journal of Nuclear Materials*, 436 (2013) 5, 68-75.
- [9] M. Kos, J. Ferces, M. Brnucko, R. Rudolf, I. Anzel, pressing of Partially Oxide-Dispersion-Strengthened Copper using the ECAP Process, *Materials and technology*, 48 (2014) 3, 379-384.
- [10] B. Mašek, O. Khalaj, Z. Nový, T. Kubina, H. Jirkova, J. Svoboda, C. Štádl, Behaviour of New ODS Alloys under Single and Multiple Deformation, *Materials and technology*, 50 (2016) 6, 891-898.
- [11] Marmy, P., Kruml, T., Low cycle fatigue of Eurofer 97, *Journal of Nuclear Materials*, 377 (2008) 1, 52–58.
- [12] M. Misovic, N. Tadic, M. Jacimovic, M. Janjic, Deformations and Velocities during the Cold Rolling of Aluminium Alloys, *Materials and technology*, 50 (2016) 1, 59-67.
- [13] A. Grajcar, Microstructure Evolution of Advanced High-Strength Trip-Aided Bainitic Steel, *Materials and technology*, 49 (2015) 5, 715-720.
- [14] B. Sustarvic, I. Paulin, M. Godec, S. Glodez, M. Sori, J. Flasker, A. Korosec, S. Kores, G. Abramovic, DSC/TG of Al-based Alloyed Powders for P/M Applications, *Materials and technology*, 48 (2014) 4, 439-450.
- [15] F. Tehovnik, J. Burja, B. Podgornik, M. Godec, F. Vode, Microstructural Evolution of Inconel 625 during hot Rolling, *Materials and technology*, 49 (2015) 5, 899-904.